Periodic Interference Structures in the Timelike Proton Form Factor

Andrea Bianconi
Dipartimento di Ingegneria dell' Informazione, Università degli Studi di Brescia and Istituto Nazionale di Fisica Nucleare, Gruppo Collegato di Brescia, I-25133 Brescia, Italy

Egle Tomasi-Gustafsson
CEA, IRFU, SPhN, Saclay, 91191 Gif-sur-Yvette Cedex, France

(Received 16 February 2015; revised manuscript received 2 April 2015; published 12 June 2015)

An intriguing and elusive feature of the timelike hadron form factor is the possible presence of an imaginary part associated to rescattering processes. We find evidence of that in the recent and precise data on the proton timelike form factor measured by the *BABAR* Collaboration. By plotting these data as a function of the 3-momentum of the relative motion of the final proton and antiproton, a systematic sinusoidal modulation is highlighted in the near-threshold region. Our analysis attributes this pattern to rescattering processes at a relative distance of 0.7–1.5 fm between the centers of the forming hadrons. This distance implies a large fraction of inelastic processes in $\bar{p}p$ interactions, and a large imaginary part in the related $e^+e^- \to \bar{p}p$ reaction because of unitarity.

DOI: 10.1103/PhysRevLett.114.232301 PACS numbers: 13.75.-n, 13.40.Gp, 14.20.-c

Electromagnetic hadron form factors (FFs) are fundamental quantities that describe the internal structure of the hadron (for a recent review, see Ref. [1]). FFs enter explicitly in the coupling of a virtual photon with the hadron electromagnetic current, and can be directly compared to hadron models, which describe dynamical properties of hadrons. They are experimentally accessible through the knowledge of the differential cross section and the polarization observables.

Traditionally, most data on FFs come from electron-proton elastic scattering. It is assumed that the interaction occurs through the exchange of a single virtual photon that carries a 4-momentum transfer squared q^2. In this kinematical region [spacelike (SL)] the virtual photon-proton coupling and the electron-proton scattering cross section are described via two real FFs, electric, G_E, and magnetic, G_M.

FFs have been also studied in the timelike (TL) region of momentum transfer squared. They are measured through the reactions

$$e^+ + e^- \to \bar{p} + p, \tag{1}$$

$$\bar{p} + p \to e^+ + e^-, \tag{2}$$

where a hadron pair is formed by or annihilated into a virtual photon. In the following we will refer to the former reaction, when not otherwise specified.

Assuming single photon exchange, the unpolarized cross section contains the squared moduli of two TL FFs (electric and magnetic FF), which are complex-valued functions of q^2. The imaginary part is expected to be large and information on the relative phase between G_E and G_M can be extracted from single spin polarization experiments [2], which are presently out of reach. In this Letter evidence for periodic structures in TL FF data is reported and related to their complex nature.

Many models for the hadron coupling to the virtual photon have been developed and applied to the calculation of SL FFs. Some of them may be analytically continued to the TL region. This is the case for approaches based on vector meson dominance [3,4] and dispersion relations [5,6]. Constituent quark models in light front dynamics may be applied [7], as well as approaches based on AdS/QCD correspondence [8]. A phenomenological picture has been recently proposed for an interpretation of FFs in both the SL and TL regions [9].

The individual determination of the electric and magnetic TLFF is obtained, in principle, from the angular distribution of reactions (1), (2), but until now the luminosity was not sufficient. The various experimental results are therefore compared on the basis of a generalized FF [10], which is related to the unpolarized cross section, σ, by:

$$|F_p|^2 = \frac{3\beta q^2 \sigma}{2\pi\alpha^2(2+\frac{1}{\tau})}, \tag{3}$$

where $\alpha = e^2/(4\pi)$, $\beta = \sqrt{1-1/\tau}$, $\tau = q^2/(4M^2)$, and M is the proton mass.

Even in these simplified terms, it has long been difficult to analyze with precision the behavior of the data over a broad kinematic range because of the uncertainties and of the matching of data from different experiments which covered limited q^2 regions. The recent data by the *BABAR* Collaboration [11,12] cover with reasonable continuity a region ranging from slightly over the $\bar{p}p$ threshold to

$q^2 \approx 36$ GeV^2. In particular, about 30 data points have been extracted in the region $q^2 < 10$ GeV^2, with a relative error lower than 10%. These features allow for a refined analysis of the systematic behavior of the TLFF, where large-scale and small-scale (in q^2 sense) properties of the data distribution may be scrutinized.

From now on, we use the expression "near-threshold region" to indicate a q^2 range extending from the threshold of the $\bar{p}p$ channel up to $q^2 \approx 9$ GeV^2 (with the convention $c = \hbar = 1$). In this kinematic region, two different scales participate: the total energy of the colliding e^+e^- pair is $> 2M \approx 1.9$ GeV, while the kinetic energy of the created $\bar{p}p$ pair is relatively small. Therefore one may expect to observe complex effects where a highly relativistic formation picture expressed in terms of quarks and gluons coexists with nonrelativistic interactions of two slow hadrons leaving the formation zone.

Proton-antiproton interactions in the near-threshold region have been studied in experiments at LEAR (see Refs. [13,14] and references therein for previous data) and more recently at AD [15]. These measurements could not separate spin channels and, as in the case of the single effective FF of Eq. (3), these data have been mostly analyzed in terms of a single effective scattering amplitude, as if proton and antiproton were scalar particles.

We define "large inelasticity" when, writing the amplitude as a sum of partial waves, at least half of the incoming flux is absorbed for all the partial waves of angular momentum L satisfying $L \leq Rp$, $R \simeq 1$ fm. The unitarity limit is reached when there is total absorption for these waves. For the inelastic cross section $\bar{p} + p \to X \neq \bar{p} + p$, large inelasticity occurs in all the kinematical range of interest here, with the possible exception of the region $p <$ 50 MeV [16,17]. For $p \gg 100$ MeV the inelastic cross section of $\simeq$40 mb is close to the black disk limit $\approx$50 mb.

As a consequence, unitarity leads to a large imaginary part in the amplitude of $\bar{p} + p \to$ *exclusive final states*, including Eq. (2). Near the threshold this is rigorously stated by Watson's final state theorem [18] applied to reaction (1). More in general, the presence of a large transition amplitude $\bar{p} + p \to A_n$, where A_n is an on-shell channel, implies a contribution to the imaginary part of the amplitude of Eq. (2) from a Cutkosky cut applied to the intermediate state of the 2-step process $\bar{p} + p \to A_n \to e^+ + e^-$.

Understanding at which extent phenomenological $\bar{p}p$ interactions could be final state interactions of the reaction (1) and seriously affect its amplitude, is, however, complicated by an evident "mismatch" of two known features of these processes:

(i) The analysis of annihilation and scattering data has shown that the colliding proton and antiproton do not overlap at small kinetic energies. As soon as these particles come close within 1 fm of each other, they either annihilate or scatter in a hard-core way [16,19]. So the wave function describing a $\bar{p}p$ state presents a "hole" of size 1 fm. Within a momentum range of 400 MeV over the $\bar{p}p$ threshold, this property is demonstrated by counterintuitive phenomena as the equality of $\bar{p}p$, $\bar{p}$D, and $\bar{p}^4$ He annihilation cross sections at small energies [16], and the suppressed effect of the electric charge in $\bar{p}$-nucleus annihilation with the paradoxical effect of $\bar{n}$ cross sections on heavy nuclei exceeding $\bar{p}$ ones [20].

(ii) In the exclusive reaction (1) quark-counting rules [21,22] predict that in the initial stages of the formation process quarks and antiquarks are concentrated in a region of size $1/\sqrt{q^2}$, which means at a relative distance of 0.1 fm when $q^2 \approx 4$ GeV^2. So, in the initial formation stages the hadrons lie at a distance that is not normally tested in phenomenological $\bar{p}p$ interactions, making rescattering effects largely unpredictable.

In order to search for signals of final state effects at small kinetic energies in the data, it is more convenient to introduce variables directly related to the relative motion of the hadron pair. In the following we will use the 3-momentum p of one of the two hadrons in the frame where the other one is at rest:

$$p \equiv \sqrt{E^2 - M^2}, \qquad E \equiv q^2/(2M) - M. \tag{4}$$

The usefulness of this variable presumes that the process can be divided into two stages: formation and rescattering, where the latter involves energies on a smaller scale than the former. This means that the amplitude for the process is the sum of a leading term due to a "bare formation" process taking place on a time scale $1/\sqrt{q^2}$, and a relatively small perturbation associated with rescattering processes taking place on a larger time scale.

A consequence of this assumption is that the measured FFs can be fitted by a function of the form

$$F(p) \equiv F_0(p) + F_{\rm osc}(p), \tag{5}$$

$$|F_{\rm osc}(p)| \ll |F_0(p)|, \tag{6}$$

$$\langle F_{\rm osc}(p)\rangle_{\Delta p} \to 0 \quad \text{for } \Delta p \gg 1 \text{ GeV}^2, \tag{7}$$

where (a) $F_0(p)$ is the translation in terms of the variable p of a known parametrization that has been adjusted on the data in the full range $4M^2 < q^2 \lesssim 36$ GeV^2 (see below) ignoring small-scale oscillations. $F_0(p)$ is regular and smooth on the GeV/c scale. We call it "regular background fit." (b) $F_{\rm osc}(p)$ reproduces GeV-scale or sub-GeV-scale irregularities in the lower part of the p range. We call it "oscillation fit." $\langle F_{\rm osc}(p)\rangle_{\Delta p}$ is the local average of $F_{\rm osc}(p)$ over the momentum range $[p - \Delta p/2, p + \Delta p/2]$.

The data by the *BABAR* Collaboration [11,12] are selected for this study since they are the most precise data in the near-threshold region and they cover with continuity a very large kinematic range. Both properties are necessary for our analysis. The fitting procedure used is the MINUIT package [23], based on the minimization of

$\chi^2 = \sum_i [f(x_i, p_i) - y_i]^2/\sigma_i^2$, where σ_i is the error on the point of coordinates (x_i, y_i) and f is the fitting function depending on the parameters p_i. The error on p_i is the interval where χ^2/n.d.f increases by one unit (n.d.f. is the number of degrees of freedom: number of points minus number of parameters).

To satisfy Eq. (7) a good choice of the regular background term $F_0(p)$ is needed. The generalized FF has been consistently extracted at $e + e^-$ colliders and antiproton facilities. It shows a decreasing behavior as a function of q^2, which was generally fitted in the experimental papers before the year 2006 with the function [24,25]:

$$|F_{\text{scaling}}(q^2)| = \frac{\mathcal{A}}{(q^2)^2 \log^2(q^2/\Lambda^2)}. \quad (8)$$

A good fit of the data prior to *BABAR*'s last results was obtained with $\mathcal{A} = 40$ GeV^{-4} and $\Lambda = 0.45$ GeV^2.

Based on Ref. [26], in order to avoid ghost poles in α_s the following modification was suggested ([27]):

$$|F_{\text{scaling+corr}}(q^2)| = \frac{\mathcal{A}}{(q^2)^2 [\log^2(q^2/\Lambda^2) + \pi^2]}. \quad (9)$$

In this case the best fit parameters are $\mathcal{A} = 72$ GeV^{-4} and $\Lambda = 0.52$ GeV^2.

In Ref. [8] a form was suggested with two poles of dynamical origin (induced by a dressed electromagnetic current):

$$|F_{T3}(q^2)| = \frac{\mathcal{A}}{(1 - q^2/m_1^2)(2 - q^2/m_2^2)}. \quad (10)$$

The best fit parameters are $\mathcal{A} = 1.56$, $m_1^2 = 1.5$ GeV^2, and $m_2^2 = 0.77$ GeV^2.

The TLFF data from the *BABAR* Collaboration [11,12] were obtained from the reaction

$$e^+ + e^- \to \bar{p} + p + \gamma, \quad (11)$$

where the photon is preferentially emitted in the entrance channel. These data, extending from the threshold to $q^2 \approx 36$ GeV^2, are well reproduced by the function [28]

$$|F_{BABAR}(q^2)| = \frac{\mathcal{A}}{(1 + q^2/m_a^2)[1 - q^2/0.71]^2}, \quad \mathcal{A} = 7.7 \text{ GeV}^{-4}, \quad m_a^2 = 14.8 \text{ GeV}^2. \quad (12)$$

The world data are shown in Fig. 1 as a function of the transferred momentum q^2, and compared with the fits from Eqs. (8), (9), (10), (12). The near-threshold region is highlighted in the inset.

In the following, we present results with $F_0(p) \equiv F_{BABAR}[q^2(p)]$. This function does not follow the expected asymptotic QCD counting rules, but best reproduces the *BABAR* data, the slope of which is steeper than $1/(q^2)^2$. It has to be considered as a local approximation of some more complicated function. We have checked that, taking any of the above background possibilities gives consistent results (within the errors) although the fit has a smaller χ^2/n.d.f. using F_{BABAR}.

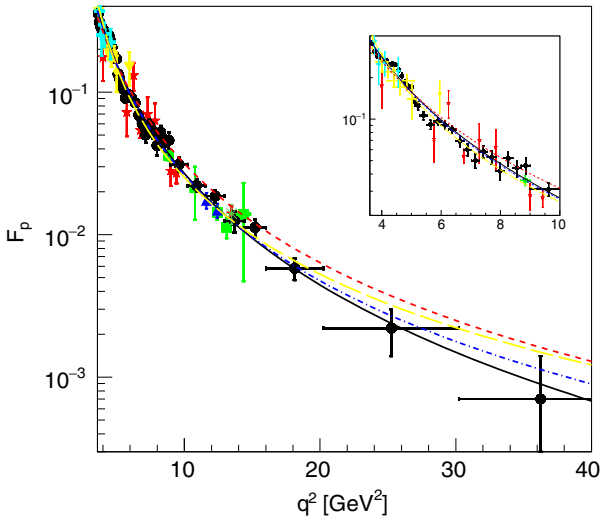

FIG. 1 (color online). World data on the TL proton generalized FF as a function of q^2, together with the calculation from Eq. (8) (blue dash-dotted line), Eq. (9) (red dashed line), Eq. (10) (yellow long-dashed line), and Eq. (12) (black solid line). The world data are from Refs. [11,12] (black solid circles), Ref. [29] (red stars), Ref. [24] (green squares), Ref. [30] (blue triangles up), Ref. [31] (yellow triangles down), Refs. [32,33] (cyan full crosses), Ref. [34] (magenta full diamonds), and Ref. [35] (dark green asterisk). The inset magnifies the near threshold region.

In Fig. 2(a) the *BABAR* data are plotted as a function of p. The result of the fit using Eq. (12) is then subtracted from the data. This difference $\mathcal{D}$ [i.e., data minus $F_0(p)$] is shown in Fig. 2(b) and exhibits a damped oscillatory behavior, with regularly spaced maxima and minima. Assuming that the first maximum is at $p = 0$, the distance between this, the 2nd and the 3rd maximum is $\Delta p \approx 1.14$ GeV. After the 3rd maximum the oscillations of the data are within the error bars.

This behavior is fitted with the 4-parameter function

$$F_{\text{osc}}(p) \equiv A \exp(-Bp) \cos(Cp + D). \quad (13)$$

The values of the parameters are reported in Table I.

The relative size of the oscillating term over the regular background is ~10%. The damping range of the oscillations of Fig. 2(b) is $1/B \approx 1.4$ GeV. $F_0(p)$ decreases by a factor $1/e$ within about 1.5 GeV. The relative magnitude of the oscillations to the regular background term $F_0(p)$ does not change much at increasing p, although increasing errors make the oscillations undetectable for $p > 3$ GeV ($q^2 > 10$ GeV^2). At asymptotically large q^2 values, the Phragmén-Lindelöff theorem [36] requires that the imaginary part of TLFFs vanishes, which implies that rescattering disappears. So, although we expect a large-momentum

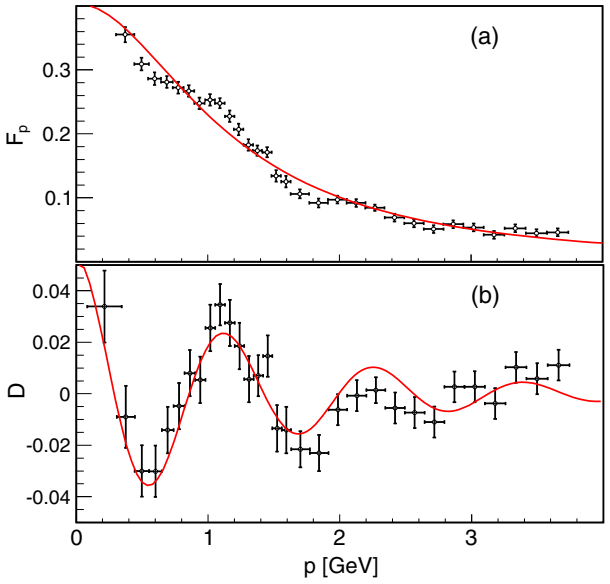

FIG. 2 (color online). (a) TL proton generalized FF as a function of p from Refs. [11,12]; the line is the regular background fit with Eq. (12); (b) data after subtraction of the fit; the line is the fit with Eq. (13).

suppression of the relative weight of the rescattering terms, this is not seen in the range $q^2 < 10$ GeV^2, where error bars allow us to distinguish systematic from statistical oscillations in the data.

The periodicity and the simple shape of the oscillations seem to exclude a random arrangement of maxima and minima of heterogeneous origin. Rather, they indicate a unique interference mechanism behind all the visible modulation. A simple oscillatory behavior in p means that the waves corresponding to the outgoing particles originate from a small number of coherent interfering sources: these waves may share a common initial source but be rescattered along different paths or in different ways so to acquire different phases. We may speak of "alternative rescattering pathways." These must be in a small number and there must be discontinuity among them, otherwise we would see diffraction patterns instead of interference patterns. For example, in Ref. [9] it has been suggested that, during the intermediate stages of $\bar{p}p$ formation, charge and color are distributed in a highly inhomogeneous way, with discontinuity features.

Since we do not know the rescattering mechanism, we cannot identify the sources of rescattered waves, but we may gain some clue on their space distribution. Let $\vec{r}$ be the space variable that is conjugated to $\vec{p}$ via three-dimensional Fourier transform. We may identify r as the distance between the centers of the two forming or formed hadrons, in the frame where one is at rest. Let $M_0(r)$ and $M(r)$ be the Fourier transforms of the regular background fit and of the complete fit:

$$F_0(p) \equiv \int d^3\vec{r} \exp(i\vec{p}\cdot\vec{r}) M_0(r), \tag{14}$$

$$F(p) = F_0(p) + F_{\rm osc}(p) \equiv \int d^3\vec{r} \exp(i\vec{p}\cdot\vec{r}) M(r). \tag{15}$$

$M_0(r)$ is shown in Fig. 3, left panel. The most relevant feature is that $M_0(r)$ decreases by 7 orders of magnitude for r ranging from 0 to 2 fm. The decrease is regular and almost constant on a semilog scale. $M_0(r)$ is steep near the origin, too. From a mathematical point of view, this follows from the fact that at the threshold of the $\bar{p}p$ channel the function $F_0(p)$ is a regular, continuous, and rapidly decreasing function of q^2. It can be interpreted by the fact that both $F_0(p)$ and its transform $M_0(r)$ are expressions of that short distance quark-level dynamics [21,22] that permits exclusive $\bar{p}p$ production at the condition that the final quarks and antiquarks are formed within a small region. Near threshold, the size of this region is ≤ 0.1 fm, much smaller than the standard hadron size.

In the right panel of Fig. 3 $M(r)$ is superimposed to $M_0(r)$. We notice that these two functions do not differ for $r < 0.7$ fm, and that the physical reason of the data oscillation must be searched for in processes taking place in the r range 0.7–1.5 fm. This range is important because it includes the distances corresponding to the largest annihilation probability in the phenomenological $\bar{p}p$ interactions in the near-threshold region [16,19,20]. At a distance of 1 fm, the relevant part of rescattering must involve physical or almost physical hadrons that annihilate into groups of 2–10 mesons. As discussed above, this means a large contribution to the imaginary part of the amplitude for

TABLE I. Fit parameters from Eq. (13).

$A \pm \Delta A$	$B \pm \Delta B$ [GeV]$^{-1}$	$C \pm \Delta C$ [GeV]$^{-1}$	$D \pm \Delta D$	χ^2/n.d.f
0.05 ± 0.01	0.7 ± 0.2	5.5 ± 0.2	0.03 ± 0.3	1.2

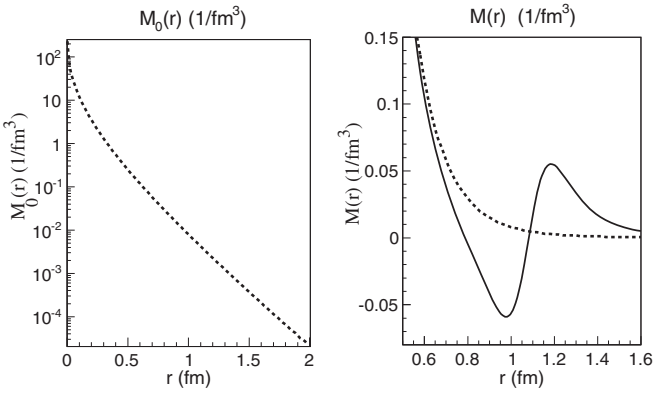

FIG. 3. (Left) $M_0(r)$, Eq. (14). (Right) $M(r)$ (solid line) from Eq. (15), and $M_0(r)$ (dashed line) for comparison (linear vertical scale).

$\gamma^* \to \bar{p}p$ from the Cutkosky cuts applied to all the two-step processes like $\gamma^* \to n\pi \to \bar{p}p$, where $n\pi$ is a state composed by n on-shell pions (or other mesons).

Rescattering with a phase shift between alternative channels may take place via formation of s-channel poles, or via t-channel photon-meson exchanges. Both classes of processes have important SL continuations. Phenomenological s-channel poles lead to nontrivial phenomena due to their imaginary parts, but not to periodic oscillations (see the analysis in Ref. [37] on the continuation of some known SL models to the TL region). Exchange of t-channel photons leads to a Coulomb phase in the TL region. In the case of photon-meson t-channel exchange, we have a large set of possibilities (e.g., $n\bar{n}$ formation followed by charge exchange). In the corresponding SL diagrams a virtual photon-meson is emitted by the nucleon before the hard vertex and reabsorbed after it. In the case of virtual photons, at large (TL and SL) $|q^2|$ this process would not be more relevant than multiple photon exchange between the nucleon and the lepton currents [38]. If the exchanged bosons are mesons, the corresponding SL diagrams modify the distribution of the proton charge. The way SLFFs are affected is strongly model dependent as shown, in particular, in the neutron case in a series of works (see Ref. [39] and references therein).

In summary, a systematic modulation pattern in the TLFF measured by the *BABAR* Collaboration in the near-threshold region has been highlighted in the range $q^2 < 10\ \mathrm{GeV}^2$. This modulation presents periodical features with respect to the momentum p associated with the relative motion of the final hadrons. It suggests an interference effect involving rescattering processes at moderate kinetic energies of the outgoing hadrons. Such processes take place when the centers of mass of the produced hadrons are separated by $\simeq 1$ fm. For this reason at least a relevant part of the rescattering must consist of interactions between phenomenological or almost phenomenological protons and antiprotons. These phenomenological reactions are known to have inelastic cross sections overcoming $1/2$ of their unitarity limit. Unitarity arguments imply the presence of a large imaginary part of TLFF. The relative errors of the data increase with q^2, making us able to detect the modulation for $q^2 < 10\ \mathrm{GeV}^2$, but its relative magnitude of about 10% is constant in this range, suggesting the interesting possibility that this modulation could be observed at larger q^2 in forthcoming more precise data. Precise measurements in the near threshold region are ongoing at BESIII (BEPCII), on the proton as well as on the neutron, bringing a new piece of information. The measurement of TL FFs in a large q^2 range will be possible at PANDA (antiProton Annihilation at Darmstadt) at FAIR (Facility for Antiproton and Ion Research).

[1] S. Pacetti, R. Baldini Ferroli, and E. Tomasi-Gustafsson, Phys. Rep. **550–551**, 1 (2015).

[2] A. Dubnickova, S. Dubnicka, and M. Rekalo, Nuovo Cimento Soc. Ital. Fis. **109A**, 241 (1996).

[3] R. Bijker and F. Iachello, Phys. Rev. C **69**, 068201 (2004).

[4] C. Adamuscin, S. Dubnicka, A. Dubnickova, and P. Weisenpacher, Prog. Part. Nucl. Phys. **55**, 228 (2005).

[5] M. A. Belushkin, H.-W. Hammer, and Ulf-G. Meissner, Phys. Rev. C **75**, 035202 (2007).

[6] E. L. Lomon and S. Pacetti, Phys. Rev. D **85**, 113004 (2012).

[7] J. de Melo, T. Frederico, E. Pace, and G. Salme, Phys. Lett. B **581**, 75 (2004).

[8] S. J. Brodsky and G. F. de Teramond, Phys. Rev. D **77**, 056007 (2008).

[9] E. Kuraev, E. Tomasi-Gustafsson, and A. Dbeyssi, Phys. Lett. B **712**, 240 (2012).

[10] G. Bardin *et al.*, Nucl. Phys. **B411**, 3 (1994).

[11] J. Lees *et al.* (BaBar Collaboration), Phys. Rev. D **87**, 092005 (2013).

[12] J. Lees *et al.* (BaBar Collaboration), Phys. Rev. **D88**, 072009 (2013).

[13] A. Zenoni *et al.*, Phys. Lett. B **461**, 413 (1999).

[14] A. Zenoni *et al.*, Phys. Lett. B **461**, 405 (1999).

[15] A. Bianconi *et al.*, Phys. Lett. B **704**, 461 (2011).

[16] A. Bianconi, G. Bonomi, M. P. Bussa, E. Lodi Rizzini, L. Venturelli, and A. Zenoni, Phys. Lett. B **483**, 353 (2000).

[17] W. Bruckner *et al.*, Z. Phys. A **335**, 217 (1990).

[18] K. M. Watson, Phys. Rev. **88**, 1163 (1952).

[19] C. Batty, E. Friedman, and A. Gal, Nucl. Phys. **A689**, 721 (2001).

[20] E. Friedman, Nucl. Phys. **A925**, 141 (2014).

[21] V. Matveev, R. Muradian, and A. Tavkhelidze, Lett. Nuovo Cim. **7**, 719 (1973).

[22] S. J. Brodsky and G. R. Farrar, Phys. Rev. Lett. **31**, 1153 (1973).

[23] R. Brun and F. Rademakers, Nucl. Instrum. Methods Phys. Res., Sect. A **389**, 81 (1997).

[24] M. Ambrogiani *et al.* (E835 Collaboration), Phys. Rev. D **60**, 032002 (1999).

[25] G. P. Lepage and S. J. Brodsky, Phys. Rev. Lett. **43**, 545 (1979).

[26] D. V. Shirkov and I. L. Solovtsov, Phys. Rev. Lett. **79**, 1209 (1997).

[27] E. A. Kuraev, private communication.

[28] E. Tomasi-Gustafsson and M. Rekalo, Phys. Lett. B **504**, 291 (2001).

[29] M. Ablikim *et al.* (BES Collaboration), Phys. Lett. B **630**, 14 (2005).

[30] M. Andreotti *et al.*, Phys. Lett. B **559**, 20 (2003).

[31] A. Antonelli *et al.*, Phys. Lett. B **334**, 431 (1994).

[32] D. Bisello *et al.*, Nucl. Phys. **B224**, 379 (1983).

[33] D. Bisello *et al.* (DM2 Collaboration), Z. Phys. C **48**, 23 (1990).

[34] B. Delcourt *et al.*, Phys. Lett. **86B**, 395 (1979).

[35] T. Pedlar *et al.* (CLEO Collaboration), Phys. Rev. Lett. **95**, 261803 (2005).

[36] E. Titchmarsh, *The Theory of Functions*, Oxford Science Publications (Oxford University Press, New York, 1939), ISBN 9780198533498.

[37] S. J. Brodsky, C. E. Carlson, J. R. Hiller, and D. S. Hwang, Phys. Rev. D **69**, 054022 (2004).

[38] E. A. Kuraev, M. Shatnev, and E. Tomasi-Gustafsson, Phys. Rev. C **80**, 018201 (2009).

[39] B. Pasquini and S. Boffi, Phys. Rev. D **76**, 074011 (2007).